7492586
BSc Neuroscience
Dr. Marcelo Montemurro

A novel computational model of neuron-astrocyte networks

0 – Abstract

An overwhelming body of evidence strongly implicates astrocytes in synaptic plasticity, information processing and intelligence. Currently, we lack a comprehensive model of how astrocytes integrate as functional elements in the learning networks of the brain. To investigate neuron-astrocyte networks, computational techniques borrowed from the field of artificial intelligence were used to create models. The aim of this project was to implement a published model and develop upon it to improve its biological plausibility. By re-implementing this model, it was found that it lacked biological validity and simulations showed that its learning performance was worse than a neural network alone, contrary to the original authors' findings. Finally, I developed my own computational neuron-astrocyte network model. Although time has limited complete refinement of the model it offers great promise as a framework for future models.

1 – Introduction

The consensus understanding of the cellular mechanisms of brain function may be reduced, albeit partially, to the following definition. The brain is a biological learning machine which stores memories as synaptic weight adjustments (synaptic plasticity; SP) to create a custom network architecture. This custom architecture is used to process novel sensory inputs (information processing; IP) to determine the motor outputs of the organism. It has been a long-held tenet of neuroscience that the cellular elements responsible for SP and IP are neurons. However, accumulating evidence since the early 1990s (1–5) has convincingly demonstrated a prominent role of astrocytes in both SP and IP (for comprehensive reviews see (6–8)). Based on this evidence, modern theories of the cellular basis of brain function are adapting to incorporate astrocytes.

1.1 – Evidence for the role of astrocytes

The recognition that astrocytes are able to both detect and release virtually all known neurotransmitters has fuelled the blooming research into astrocytes as functional components of the synapse (6,9–12). This is called the tripartite synapse which digresses from the traditional view of a synapse as it accommodates for the communicative capacity of a perisynaptic astrocyte. Neurotransmitter released by presynaptic neuron may bind to receptors on the astrocyte and lead to its activation (9,13–15)**.** In an active state, astrocytes may release neurotransmitters or other chemicals back to the synaptic cleft contributing to the total neurotransmitter detected by postsynaptic neuron. (16–19) Furthermore, astrocytes may communicate with other astrocytes (4,20–25). I will now briefly summarise the current understanding of the role of astrocytes in IP and SP.

1.1.2 – Astrocyte activation and information processing

Astroyctes possess a diverse repertoire of ionotropic and metabotropic receptors. (10,12,13) These receptors often mirror the receptors found on the postsynaptic neuron, thus facilitating the processing of synaptic activity. (10,12,13) Importantly, each astrocyte is associated with a unique population of synapses and therefore integrates a unique set of inputs (26). Persistently high levels of synaptic activity may activate the astrocyte (11,19,27,28). It is widely-accepted that astrocytes represent their activation in the form of spatio-temporally complex calcium (Ca^{2+}) responses (11,19,27–29). These

Ca^{2+} responses are built from two fundamental types of subcellular Ca^{2+} events. Type 1 events, sometimes called focal-transient microdomains, are high frequency, short-lasting Ca^{2+} events confined to areas of up to 4 μm (16). Type 1 events are caused by spontaneous sub-threshold presynaptic neurotransmitter release (16). Conversely, type 2 events are initiated by the occasional coincident arrival of multiple action potentials at synapses contained within the astrocyte's domain to form longer-lasting and larger Ca^{2+} events (16,27,30).

The predominant molecular mechanism for the generation of Ca^{2+} events is known to involve inositol 1,4,5-trisphosphate (IP3)-mediated release of Ca^{2+} stores from the endoplasmic reticulum (ER) (15,28,31). These local Ca^{2+} events may propagate down the processes of the astrocyte to form intracellular Ca^{2+} waves (15,32,33). The formation of an intracellular Ca^{2+} wave is dependent on the interplay of multiple parameters. These parameters include ratios of Ca^{2+} buffering, extrusion and amplification, as well as levels of IP3 degradation and production enzymes, reviewed in references (12,19,32,34). In some cases, these intracellular Ca^{2+} waves may develop into whole-cell Ca^{2+} responses. Whole-cell Ca^{2+} responses have a characteristic initial Ca^{2+} peak at approximately 1-2 seconds (30) post stimulation followed by either a plateau phase or sustained Ca^{2+} oscillations. They finally return to baseline levels at approximately 7-30 seconds (7,30,35) after stimulation. Such a temporal scale contrasts that of neurons by several orders of magnitude. Ca^{2+} oscillations are thought to encode information through their amplitude and frequency as well as characteristic oscillation patterns. (7,28,36,37) Decoding these patterns is an area of active research (15,38,39).

The complexity of Ca^{2+} encoding is further expanded by the capacity of Ca^{2+} waves to propagate to neighbouring astrocytes via gap junctions to form intercellular Ca^{2+} waves (ICWs) (4,13,23,35). Gap junctions act as simultaneous input-output portals between astrocytes, permitting intercytoplasmic transfer of molecules less than 1 kDa (23). The speed of ICW propagation is slow (16 μm/sec) and fairly uniform across the literature (32,40–42). Conversely the degree of coupling between astrocytes in different regions of the brain can vary significantly (26). Some ICWs are reported to recruit 2-5 astrocytes (42,43) whereas other groups report ICWs involving tens to hundreds of astrocytes (41,44). It may be hypothesized that astrocytes comprise three orders of IP in the brain. Most low-level is that of subcellular microdomains, followed by whole-cell responses and most high-level is that of ICWs. The integrative capacity of astrocytes is somewhat perplexing since each astrocyte may integrate tens of thousands of synapses and hundreds of other astrocytes over several seconds. This capacity of astrocytes is capitulated by **Fig. 1**.

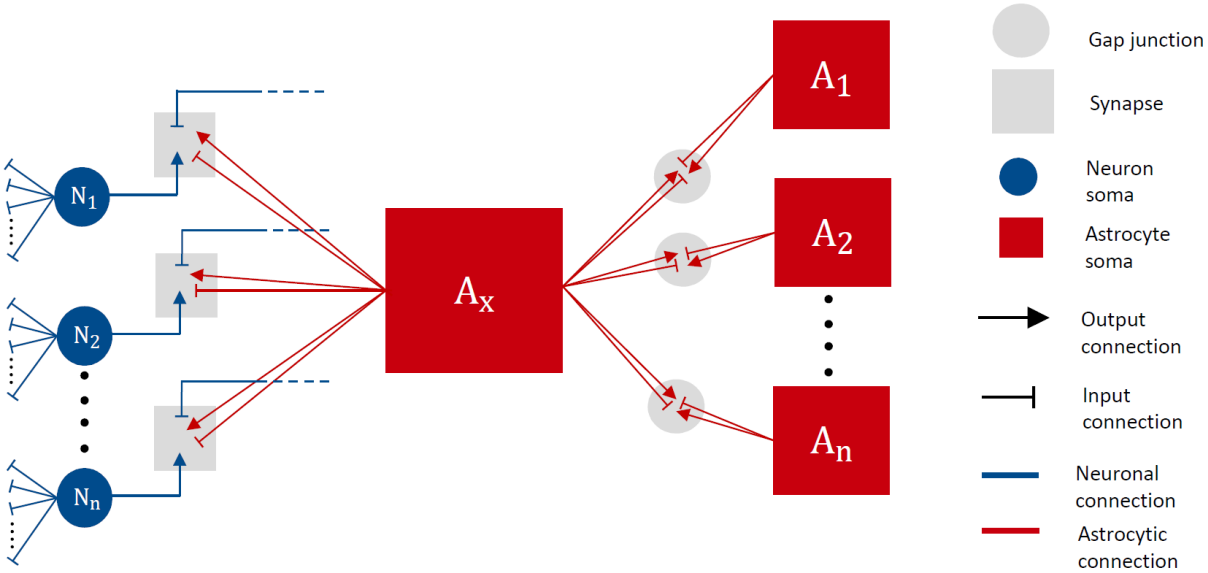

Figure 1 | Schematic of astrocytic input and output connections. A single astrocyte ireceives input from multiple synapses in its domain (up to 2 million in human brain (18)) and also from many other astrocytes via gap junctions. It is also able to output and influence the activation of these synapses and astrocytes to which it is connected.

1.1.3 – Astrocyte output and synaptic plasticity

As previously mentioned, astrocytes are capable of communicating with each other via ICWs and influencing synaptic transmission. Astrocytes have been observed exocytosing a large range of molecules including growth factors, neuropeptides and most major neurotransmitters (glutamate, GABA, acetylcholine and dopamine) (11,18,29,45–54). Furthermore, neurotransmitter clearance is heavily reliant on astrocytic uptake. At glutamatergic synapses, for example, astrocytes uptake approximately 80% of glutamate released by the presynaptic neuron (18,55,56). Thus, neurotransmitter clearance presents another viable means of regulating neurotransmission.

Astrocytic transmitter release commonly induces slow inward currents (SICs) which promote neuronal synchrony and lasts several hundred milliseconds (28,45,46,57–62). Astrocyte-induced SICs have been described in the hippocampus (45,58), cortex (42), thalamus (63), nucleus accumbens (64) and spinal cord (46). When modelling networks, important features of SICs to consider are that they may affect many neurons at once and their effects last over many synaptic events.

Astrocytic release of signalling molecules has been implicated in the four major forms of SP: short term potentiation (29,33,44,45,58,65,66), short term depression (67,68), long term potentiation (LTP) (29,33,50,67,69–72) and long term depression (LTD) (60,68,73–75). For example, D-serine stands out as a particularly good advocate for the involvement of astrocytes in LTP and LTD, due to its interaction with the NMDA receptor (NMDAR). The NMDAR is famous for its Hebbian-like “coincidence detection” of presynaptic and postsynaptic activation in LTP and LTD (76,77). However, it is often overlooked that NMDAR activation also requires the binding of a co-agonist either glycine or D-Serine (76). Findings reveal that in the mammalian brain this co-agonist is predominantly D-Serine (78) and that the predominant source of D-Serine is astrocytes (7). Therefore, NMDARs may act as coincidence detectors of presynaptic neuron, postsynaptic neuron and perisynaptic astrocyte. Indeed, experiments demonstrate that astrocytic D-Serine can gate the induction of LTP (33,50,69,71) and LTD (74,75) in a concentration-dependent manner. Other experiments (69–71) suggest a more direct involvement of

astrocytes. For example, clamping of cytoplasmic Ca^{2+} in hippocampal astrocytes was shown to prevent the formation of LTP (69).

1.3 – Modelling Astrocyte Networks

As discussed above, there is sufficient evidence to implicate astrocytes in SP and IP and therefore the complex learning and behaviours performed by brain. The brain allows for its complex learning and behaviours by the arrangement of its cells in a network. As can be seen by the comparison of species, a more complex network can often facilitate more complex behaviours. (18) Our understanding of how neuron-astrocyte networks communicate to facilitate such faculties is lacking. To investigate this problem, this project involved the implementation of artificial neural network (ANN) models. ANNs are a branch of the multidisciplinary field of artificial intelligence (AI). ANNs have been chosen as the basis for the models in this project as they consist of relatively abstract representations of cells. Thus ANNs, facilitate the exploration of the network properties that mediate learning rather than a focus on the internal cellular representation. A further justification for the use of ANNs is the strong relationship between astrocytes and intelligence. Humans show the greatest asrtocyte-to-neuron ratio, largest astrocytes and most morphologically complex astrocytes of all organisms (18). Furthermore, humans are known to possess subtypes of astrocytes unique to primates and even subtypes unique to humans (79). A recent experiment demonstrated that the transplantation of human astrocytes into mice improved the learning and memory performance of the mice (80). It is therefore somewhat surprising that there have been so few AI groups modelling neuron-astrocyte learning networks. Perhaps, this is in part due to the highly integrative properties of astrocytes (**Fig. 2**) which make them difficult modelling subjects. Neurons make good modelling subjects due to their discreteness. For example, neurons have clearly designated input and output compartments by way of dendrites and axons, respectively. In astrocytes, there are fewer constraints as perisynaptic processes and inter-astrocytic gap junctions may be considered simultaneous input and output connections (20,44). Despite these challenges, this project proposes the most important criteria for modelling neuron-astrocyte networks, as shown in **Box 1**.

Box 1 | Astrocyte criteria for modelling cellular learning in neuron-astrocyte networks

1. Each astrocyte monitors a distinct subset of synapses.
2. Activation of astrocytes is several orders slower than that of neurons.
3. The effects of astrocytes are longer-lasting than those of neurons.
4. Astrocytes are able to communicate with each other.
5. Astrocytes outnumber neurons.

One AI group at the University of Coruna has experimented in merging astrocytes with ANNs (81,82). Their model, which will be referred to as the Porto-Pazos model (PPM), claims to model the larger temporal scale of astrocytes with the result that the PPM has a better learning performance than a network consisting solely of neurons (81,82). Furthermore, this performance could not be matched by the addition of more neurons (81). The PPM therefore presents a suitable model for future models to develop upon and will serve as a foundation for this project.

1.5 – Motivation and objective

As has been reiterated throughout the literature review and introduction, astrocytes are strongly implicated in both IP and SP. However, our understanding of how astrocytes integrate as functional elements in the networks remains incomplete. Therefore, the gaps in our understanding of the cellular networks of the brain is exposed as vastly greater than most neuroscientists believe. Hebbian principles of neuronal pairing have served as a framework from which the majority of research concerned with cellular learning in neuroscience, psychology and AI have been built. The primary objective of this research was to develop a model which offers a novel, biologically plausible and mathematically permissible framework for the cellular functioning of networks in the brain. It can be hypothesized that the addition of astrocytes to ANNs will greatly enhance their learning performance. The implications of such a model are potentially great. Thomas Kuhn proposed that the progression of scientific fields do not follow continuous linear change but undergo periodic “paradigm shifts” (83). One may hypothesize that neuroscience is on the brink of such a paradigm shift: the acceptance of astrocytes as functional elements in intelligent systems. A model which fulfils the objectives of this project could induce such a paradigm shift. Furthermore, the implications of a network which outperforms ANNs are diverse and influential. ANNs are not just models of the brain but can be found to underlie a wide range of systems. For example, ANNs are used in stock market predictions (84), voice recognition (85), face recognition (86), robotics (87) and medical diagnosis. Even Google depends on ANNs for its web crawlers (88).

The project itself consisted of two parts and three specific aims. The first part of this project was to reimplement the PPM. The second part was the development a novel model. The first aim was to verify the biological and computational validity of the PPM. The second aim was to create a model which is more biologically plausible than the PPM and fulfils the criteria in **Box. 1**. The final aim was that the novel model has better learning performance than both the PPM and an unadulterated ANN.

2 – Methods

Three different ANNs were implemented in this project. The first is a generic ANN, which will be referred to as the base neural network (BNN). The second is the PPM and finally my own interpretation of an artificial astrocyte-neuron network. The PPM and my model are extensions of the BNN. In this section, an introduction to ANNs and genetic algorithms will be given, thus explaining the computational methods of the BNN. Also in this section, the implementaiton details of the PPM will be given. In the results, the implementation details of the resulting novel model will be given.

2.1 – Base neural network model

ANNs provide an approach to understanding how circuits of connected neurons may produce complex learning and behaviours. ANNs learn by example, that is they are trained by sequential presentation of samples from the dataset. The learning algorithm recognizes patterns in the dataset and stores these as modifications of the network's interconnection pattern. The dataset is generally split into training and test data. The training data is used for the learning phase of the algorithm whereas test data is used for performance assessment of the network. The datasets used in this

project were the XOR, parity and Iris datasets. XOR is the simplest dataset and consists of 4 samples each with 2 binary inputs (2-bit) coupled to a single binary target. The XOR was used for preliminary testing of the networks (data not shown). XOR was chosen as it is a small and commonly used dataset thus allowing for fast debugging of the network. The parity and Iris datasets were used in the simulations to assess the networks. The parity dataset is an extended 4-bit version of the XOR dataset for which 75 samples were generated for the training data and 75 samples for the test data. The parity dataset was chosen as it is commonly used for the assessment of ANN performance (89). The Iris dataset is real data from that of 150 measurements of flower dimensions of 3 closely related flower species (90). Each sample in the Iris dataset consists of four inputs (sepal length, sepal width, petal length and petal width) and a target which can be one of the three species. The Iris dataset was chosen for comparison purposes as it was also used by the PPM publications (81,82). As in the PPM publications the Iris dataset was split in half for training and test data.

An ANN is an abstract mathematical representation of a population of neurons connected by synaptic weights. Synaptic weights are parameters that determine the strength of the connection between presynaptic neuron and postsynaptic neuron. Adjustment of these parameters by the learning algorithm facilitates recognition and classification of patterns in the datasets. There are enumerable types of ANNs each of which can be defined by three principle properties: neuronal activation function, network architecture and learning algorithm.

2.1.1 – Neuronal activation function

The neuronal activation function determines how neurons integrate their inputs. The prototypical biological neuron is depicted by **Fig. 2A**. In simple terms, a neuron integrates its afferents over time and if the neuron reaches a particular threshold it will fire. Models of the internal operations of the neuron can vary enormously in their level of detail. For example, models like the Hodgkin-Huxley model incorporate features as low level as the changes in ionic currents (91). A commonly used model is that of a leaky-integrate and fire (LIF) neuron represented by **Fig. 2B**.

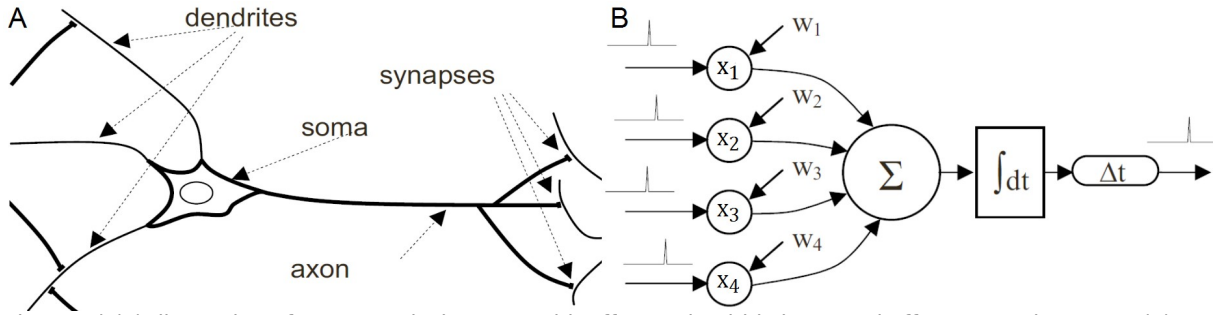

Figure 2 | (A) Illustration of a prototypical neuron with afferent dendritic input and efferent axonic output. (B) Illustration of leaky integrate and fire model. Inputs (x1-4) are multiplied by their respective synaptic weights (w1-4), summed and integrated over time. If the integral exceeds a threshold, the neuron fires and the integral is restarted. The strength of a particular synapse is indicated by the magnitude of the synaptic weight value. The delay of signal propagation along the axon may be modelled by a time parameter Δt. Adapted from (110)

The neural network models in this implementation use two types of neuron models: the threshold neuron and the hyperbolic tangent neuron. These two neuron models were chosen to match the models used in the original PPM, allowing for comparison of performance results (81,82). The boundary conditions of the output of a threshold neuron O_j are determined by neuronal threshold value θ, as given by **Eq. 1**.

$$O_j = \begin{cases} 1 & \text{if } \sum_{i=1}^{n} x_i w_{ij} > \theta \\ 0 & \text{if } \sum_{i=1}^{n} x_i w_{ij} \leq \theta \end{cases} \quad (1)$$

O_j is the postsynaptic neuron which receives inputs from presynaptic neurons represented by the vector x of length n (where n is the number of presynaptic neurons) which are multiplied by their respective synaptic weights, w. w is a matrix of values which contain the synaptic weights connecting pre- and postsynaptic neurons i and j, respectively. The hyperbolic tangent neuron is similar to a threshold neuron, however instead of gating the output of the neuron with a threshold the summed inputs are parsed through the hyperbolic tangent function as given by **Eq. 2**.

$$O_j = tanh\left(\sum_{i=1}^{n} x_i w_{ij}\right) \quad (2)$$

The hyperbolic tangent function outputs continuous values between -1 and 1 in a non-linear fashion. We apply this function to model the firing rate of the neuron. From a practical perspective, this is also important in facilitating learning of data which is not linearly separable.

2.1.2 – Interconnection pattern

As noted earlier, networks are important in biology to facilitate complex behaviours. A practical demonstration of this can be shown by using a simple classification problem such as the negative patterning problem or as it is commonly known in computer science the XOR problem (92). This problem requires a network of neurons and cannot be solved by a single neuron. In a network the pattern is represented in distributed fashion across many neurons which facilitates more complex pattern recognition.

Neurons can be connected with each other in many different architectures and there are many types of networks for example, Hopfield networks (93), Evolino networks (94) and deep belief networks (93). The models in this project will use feedforward networks (FFNs), where information flows in one direction from input layer, to hidden layer, to output layer, as shown by **Fig. 4A**. FFNs have a variable number of hidden layers and each hidden layer has a variable number of neurons. The number of neurons in the input and output layers are determined by the dimensions of the training data used. In the case of our networks used for parity and Iris datasets, we used an architecture of 4, 6 and 3 for input, hidden and output layers respectively. The output layer was a threshold layer with a θ of 0.5 and the others were hyperbolic tangent layers. These parameters were chosen to match PPM publications (81,82).

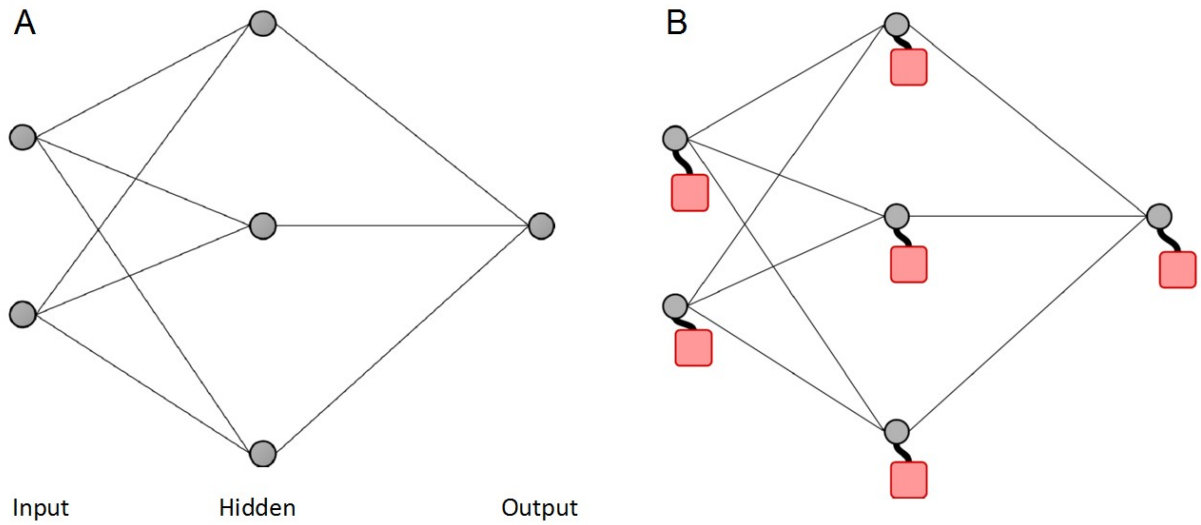

Figure 3 | Schematic of BNN and PPM architecture for the XOR dataset. Note that for the parity problem and Iris dataset the architecture would 4, 6, 3 for input, hidden and output layers respectively. (A) Representation of BNN. Input, hidden and output layers are labelled in parallel to their respective layers. Grey circles represent neurons. Thin black lines between neurons represent synaptic weights. (B) Representation of Porto-Pazos model. Red squares represent astrocytes. Thick black lines between neurons and astrocytes represent an association between neuron and astrocyte (note thick black lines do not have weight values.

2.1.3 – Learning algorithms

In biological systems, synaptic plasticity is considered the underlying mechanism of learning. The computational analogue of SP in ANNs is the modification of synaptic weight values. Learning algorithms are used to update these weights such that the output of the network is optimized to the target values for the inputs of the dataset. Given a dataset of the form $(inputs, target), inputs \in I, target \in T$ a learning algorithm seeks the function $\phi : I \rightarrow T$ where ϕ is the output of the network.

There are two main types of learning algorithms: supervised and unsupervised. Supervised learning uses the network error, calculated as the difference between output layer and target values, to adjust the synpatic weight values. Unsupervised algorithms, however, do not use the error score**.** The underlying algorithm for the models is a supervised genetic algorithm (GA). It is important to clarify that genetic algorithms bare no relation to the genetics of the cells being modelled. Rather GAs can be considered a general optimization algorithm not biologically related to the models. GAs are a branch of AI which model the supreme intelligence that created intelligent organisms: evolution (96). As in evolution, an initial population is created from which only the fittest individuals survive to generate a new population. The new generation is different from the previous population due to mutation and crossover of the genetic material. Subsequently, the process loops and the fittest individuals from this population survive to reproduce. The steps of a GA are summarised by **Fig. 3**. In our case, the initial population created is a population of neural networks (**Fig. 3.1**). We rank the fitness of the individuals by assessing their percentage error (PE) given by,

$$PE = \frac{100}{|Pat|} \cdot \sum_{<inputs,target> \in Pat} \begin{cases} 0 & \text{if } \phi(inputs) = target \\ 1 & \text{if } \phi(inputs) \neq target \end{cases} \quad (3)$$

where ϕ returns the output of the network produced by activating the network with the given inputs

and Pat is the training data used which consists of a list of samples (**Fig. 3.2**). We use PE rather than the more widely-used mean squared error, as our outputs are boolean and therefore PE provides more useful data about performance of the individual. The fitness of each individual is given by

$$fit_i = PE_i \div \sum_{j=0}^{n} PE_j \tag{4}$$

such that each fitness value is a proportion of the total PE of the population where i indicates the current individual and n denotes the population size, thus creating a probability distribution proportional to PE. Based on this probability distribution we select two individuals from the population, known as roulette wheel selection (**Fig. 3.3.1**). In the next step (**Fig. 3.3.2**) the weights of these two individuals may be crossed over if a randomly generated number falls under the crossover probability. To match PPM publications, I implemented one-point crossover and crossover probability was set to 0.9 (81). Crossover is analogous to genetic recombination of biological chromosomes, where the chromosomes are the weights of the networks. Subsequently, mutation probability determines the probability that any given weight will be randomly modified (**Fig. 3.3.3**). Again, to match PPM publications, mutation probability was set to 0.1 (81,82). Each time mutation and crossover (processes **Fig. 3.3.1-3**) are repeated, two new individuals are created and appended to the growing new population. These processes are repeated until the new population size has reached 150. Subsequently, the new population is ranked in order of fitness, thus completing the cycle. This cycle was repeated 1000 times for each trial. To evaluate the performance of the networks, the training data and test data were used to calculate the PE after these 1000 cycles.

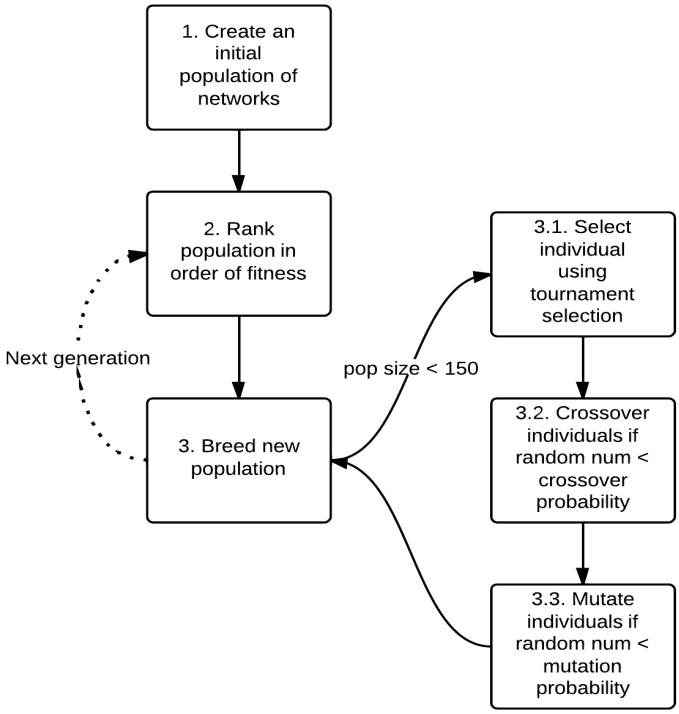

Figure 4 | Schematic of genetic algorithm. See text for explanation

2.2 – Porto-Pazos model

The PPM develops upon the BNN by including a second phase to each learning step. The first phase is an unsupervised algorithm, called the neuroglial algorithm (NGA) and the second phase is the GA described above (81,82). In the NGA, each neuron has an associated astrocyte (A) as shown in **Fig. 4**. To model the slower temporal scale of astrocytes, each sample is processed over several iterations A^{proc}. During these iterations the astrocytes activity is updated (**Eq. 5**).

$$\Delta A_j^{act} = \begin{cases} 1 & \text{if } O_j > 0 \\ -1 & \text{if } O_j \leq 0 \end{cases} \tag{5}$$

where $j \in [1, ..., Layerdim]$, $Layerdim$: number of neurons in layer, O_j : output of neuron, ΔA_j^{act} : change in astrocyte activity. If during A^{proc}, A_j^{act} reaches threshold (A^{thresh}) due to persistent neuronal activity the status of the astrocyte (A_j^{stat}) is set to 1 (positively active) or -1 (negatively active) shown by **Eq. 6**.

$$A_j^{stat} = \begin{cases} 1 & \text{if } A_j^{act} = A^{thresh} \\ -1 & \text{if } A_j^{act} = -A^{thresh} \end{cases} \tag{6}$$

If the astrocyte is activated it remains active for A^{dur} iterations and while active all presynaptic weights to the neuron j will be updated (**Eq. 7**).

$$\Delta w_{ij} = \begin{cases} w_{ij} \cdot \alpha & \text{if } A_j^{stat} = 1 \\ w_{ij} \cdot -\beta & \text{if } A_j^{stat} = -1 \end{cases} \tag{7}$$

where w_{ij} is the presynaptic weight from neuron i to j, α : 0.25, β : 0.5. In the case of the hidden layer astrocytes will not just modify all presynaptic weights of neurons in this way but also all output weights of neurons in this way. In the case of the input layer, only output weights will be modified. Finally, in the case of the output layer, only the presynaptic weights will be modified. The values for the above parameters were as follows: A^{proc}=6, A^{thresh}=3, A^{dur}=3.

2.3 – Statistical and technical details

For each model a simulation was run. Each simulation consisted of 20 trials. Each trial consisted of 1000 generations. As mentioned, for the PPM each generation consisted of the NGA followed by the GA whereas for other models each generation only involved the GA. To assess the learning performance of the various models, PE was calculated using **Eq. 3**. One-way ANOVA was chosen to compare the mean PE between all groups. Tukey test was used as a post-hoc test between groups as the results data is parametric. One-way ANOVA Tukey tests were performed using the stats module from the scipy python library. All implementations were built in python using scipy library. All simulations were run on Linux, Intel® Core™ i7-3517U with DDR3 1600MHz 4GB RAM. Speed of simulations was measured as the time taken to complete one learning epoch, as measured using the timeit module from python. Speed was measured by averaging 20 learning epochs whilst training to the Iris dataset.

3 – Results

This project has two main results sections. In the first section, the details of the proposed model will be described. In the second section, the results obtained for the learning performance of the various models will be described.

3.1 – The proposed model

The primary objective of the reciprocal astrocyte processing (RAP) model is to improve on the biological realism of the PPM. The principal difference between the PPM and the RAP model is that astrocytes in the RAP model are not part of the learning algorithm but rather assemble alongside neurons as complementary components of a united structure. Consequently, activation of the network differs from that of a traditional FFN. I will now describe RAP model activation and architecture.

For simplicity, astrocytes in the RAP model only communicate with synapses from the input layer to the hidden layer. Each astrocyte monitors a distinct subset of synapses such that astrocytes have non-overlapping domains. The number of astrocytes ($Astrodim$) is equal to the number of neurons in the hidden layer and the number of synapses in each domain are equal to the number of neurons of the input layer ($Indim$). The configuration of astrocyte-to-synapse coupling is assigned randomly and conserved during learning. To resemble gap junction coupling, all astrocytes are reciprocally connected to each other. The architecture of a simple RAP model network is illustrated by **Fig. 8A**.

Astrocytes interact with synapses in their domain via two weights. A weight from the presynaptic neuron to the astrocyte ($Synout$) and a weight from the astrocyte to the synapse ($Synin$). $Synout$ represents the capacity of neurotransmitter released from presynaptic neuron to activate receptors on the astrocytic membrane. $Synin$ represents the relationship between astrocyte activity and the probability that neurotransmitter will be released by the astrocyte at that synapse. This configuration of weights resembles the tripartite synapse (6,11) and is best represented by **Fig. 8B**. The postsynaptic neuron j subsequently sums the input from the synapse (presynaptic and astrocytic contributions included) multiplied by a third weight (w_{ij}). Therefore the activation function for the postsynaptic neuron (O_j) is modified from **Eq. 2** as follows

$$O_j = tanh\left(\sum_{i=1}^{Indim}(x_i + Aout_{ij}) \cdot w_{ij}\right) \tag{8}$$

where $Aout_{ij}$ is the output from the astrocyte to the synapse ij, where i and j are indices. $Aout_{ij}$ is combined with the output from presynaptic neuron (x_i) and multiplied by the weight w_{ij}. $Aout_{ij}$ is calculated as follows

$$Aout_{ij} = Synin_{ij} \cdot A_k \tag{9}$$

where the activity of the astrocyte is represented by A_k where $k \in [1, ..., Astrodim]$. The astrocyte's activity is dependent on three factors, shown by **Eq. 10**. Firstly, the input from the presynaptic neurons in the domain of the astrocyte (Ain). Secondly, any residual activation from previous stimuli (Lag). Finally, the astrocyte integrates from adjacent astrocytes ($Inter$).

$$A_k = tanh\left(Lag + Ain + Inter\right) \tag{10}$$

We use the hyperbolic tangent function to approximate a non-linear summation of inputs. Lag is

calculated as the mean of the astrocyte's activity over the previous τ iterations multiplied by the momentum factor γ, given by

$$Lag = \left(\frac{1}{\tau} \sum_{i=1}^{\tau-1} A_k^{t-i} \right) \cdot \gamma \tag{11}$$

where t denotes the iteration such that when $i = 0$, A_k^{t-i} refers to the activity value of the astrocyte at the current iteration, in other words $A_k^t = A_k$. For the simulations, τ was set to 3 and γ was set to 0.1. The input to the astrocyte from the presynaptic neuron is given by

$$Ain = \sum_{<i,j> \in S_k} x_i \cdot Synout_{ij} \tag{12}$$

where x represents the activity of the presynaptic neuron and S_k is a list of tupled indices which indicate the synapses monitored by the astrocyte A_k, hence $S_k = \{(i,j), ...\}$ such that $|S_k| = Indim.$ The summation of an astrocyte's reciprocal connections to other astrocytes is given by

$$Inter = \sum_{\substack{l=1 \\ l \neq k}}^{Astrodim} A_l \cdot G_{kl} \tag{13}$$

where G_{kl} represent the bidirectional gap junction weight connecting astrocytes A_k and A_l.

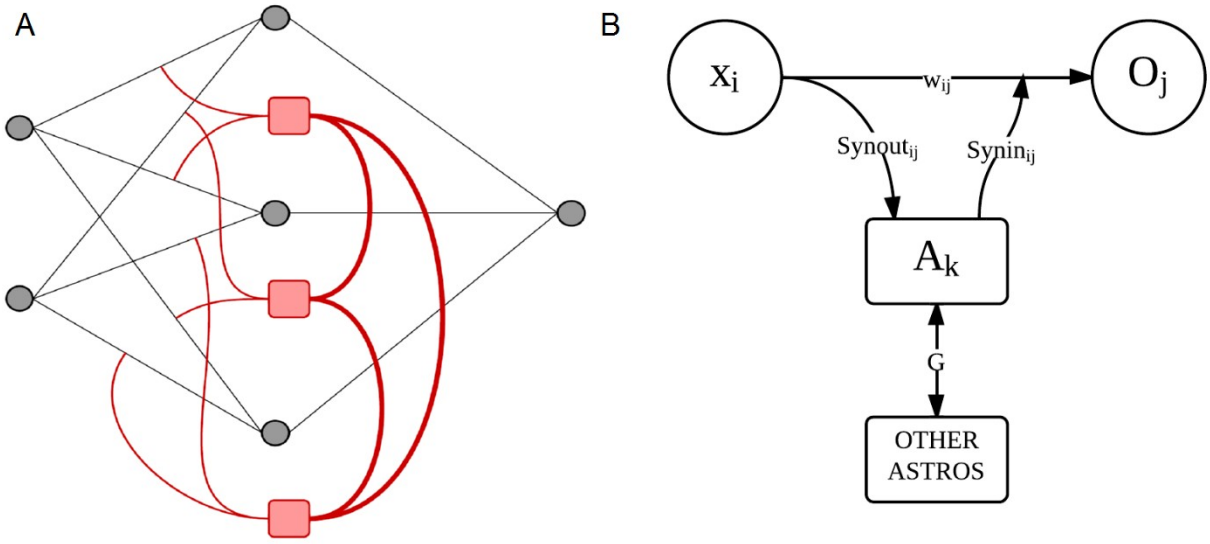

Figure 5 | (A) Schematic of RAP model architecture. Neurons depicted as grey circles and astrocytes as red squares. Black lines represent synaptic connections. Thin red lines represent astrocyte-to-synapse configuration. Note that each thin red line contains two weights namely $Synin$ *and* $Synout$*. Thick red lines represent reciprocal connections between astrocytes termed* G*. (B) Schematic of a single synapse in the RAP model.* $Synout$ *connects presynaptic input* x_i *to astrocyte* A_k *which processes this input with other inputs from other synapses. Astrocyte* A_k *also receives reciprocal input from other astrocytes (astros), via independent weights (*G*). Inputs from* Lag *and other synapses to* A_k *are not shown.* A_k *outputs back to the synapse via* $Synin$ *are not shown for clarity. The presynasptic and astrocytic contributions are then combined and detected by postsynaptic neuron via* w_{ij}*. This synaptic input ultimately contributes to the output of postsynaptic neuron* O_j*.*

The sequence of activation of the RAP network is as follows:

1. Activate the input layer.
2. Update astrocyte activity from presynaptic activity. **Eq. 12**
3. Update astrocyte activity from residual lag. **Eq. 11**

4. Update astrocyte activity from reciprocal connections with other astrocytes. **Eq. 13**
5. Update synaptic input to postsynaptic neurons from astrocytic activity. **Eq. 9,10**
6. Activate the postsynaptic hidden layer. **Eq. 8**
7. Activate the output layer. **Eq. 2**

A GA was used to train the weights of the network. The parameters used for the GA were identical to those described for other models. However, unlike in the BNN and PPM, not only neuronal weights were trained by the GA but also $Synin$, $Synout$ and G values were used as substrates for learning. During training samples were presented randomly to prevent network training to sample sequence.

3.2 – Simulations

All implementations depended upon the underlying GA of the BNN. Therefore, it was important to verify its performance. As a preliminary test, the BNN was trained to the XOR dataset. Over 20 trials, the BNN invariably achieved 0% error within 10 iterations. Subsequently, the BNN was tested on the parity dataset. The parity dataset is an extension of the XOR dataset and is commonly used for the validation of neural networks (89). The BNN was able to learn the parity dataset and achieved a test error of 1.3 % ± 0.0, averaged over 20 trials, **Fig 6A,B**. Finally, the BNN was trained to the Iris dataset, **Fig 6C,D**, where it reached a test error of 9.6 % ± 2.0. The Iris dataset was used for comparison purposes as the PPM publications used the Iris dataset (81,82).

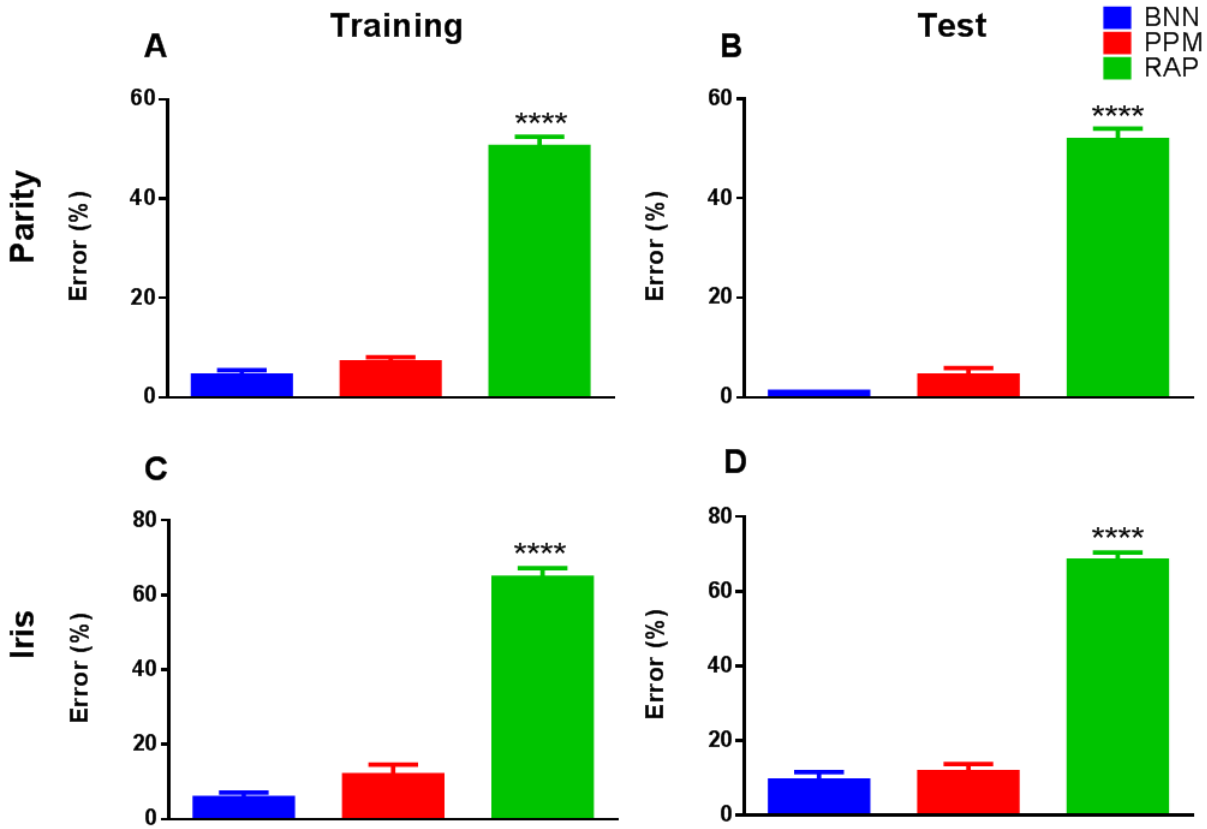

Figure 6 | Learning performance of BNN, PPM and RAP model. (A, B) Learning performance of models trained with the parity dataset. BNN (blue) and PPM (red) final training and test error are not significantly different from each other. RAP model performs significantly worse than BNN and PPM. (C, D) Final training and test error for models trained to Iris dataset. BNN and PPM scores are not significantly different from each other. RAP model performs significantly worse than BNN and PPM

To asses the performance of the PPM, the PPM was also trained to the parity and Iris datasets. **Fig. 5** shows that PPM performed similarly to the BNN in these simulations. Crucially, the Tukey post-hoc test revealed that there was no significant performance difference between PPM and BNN. The statistical results for all one-way ANOVAs and post-hoc tests can be found in **Table 1**.

*Table 1 | Statistical results of One-way ANOVA F-test and Tukey HSD post-hoc test. **** denotes a significance p-value < 0.0001. ns denotes that the difference between groups was not significant. Training refers to final training percentage error and test refers to test percentage error.*

	1. Parity Training	2. Parity Test	3. Iris Training	4. Iris Test
One-way ANOVA	****	****	****	****
BNN vs PPM	ns	ns	ns	ns
BNN vs RAP	****	****	****	****
PPM vs RAP	****	****	****	****

Fig. 6 shows the speed of the models. The PPM is approximately 6 times slower than the BNN. Also included in **Fig.5, 6** and **Tab. 1** are the results for the RAP model. As can be seen by **Fig.5** and **Tab. 1** the RAP model did not learn either datasets well and performed significantly worse than the other models. However, the results for the RAP model should be interpreted as preliminary data and do not necessarily mean that the RAP model lacks any capacity to learn. There are many parameters which require investigation, which will be discussed in greater detail in the discussion. The more important result to notice is that PPM and BNN performances are not significantly different from each other.

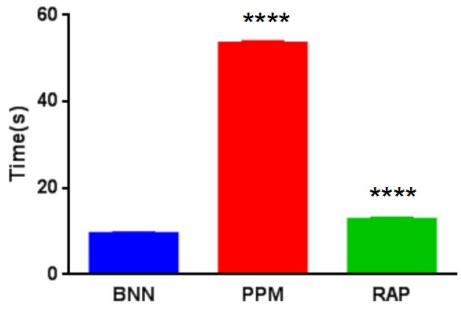

Figure 7 | Speed of one generation using the Iris dataset.

Fig. 8 shows the potential paths of astrocyte activity during the processing of a single sample. Here it is shown that while astrocyte activity can take one of eight different paths, the astrocyte will invariably reach a status of 1 (positively active, **Fig. 8 A**) or -1 (negatively active, **Fig. 8 B**) at iteration 4. Once active this status is invariably persists for the remaining processing iterations of the sample. For clarity, I will restate the meaning of astrocyte status. If the astrocyte is positively active the astrocyte is increasing its associated neuron's input weights by 25%. If the astrocyte is negatively active the astrocyte is decreasing its neuron's input weights by 50%.

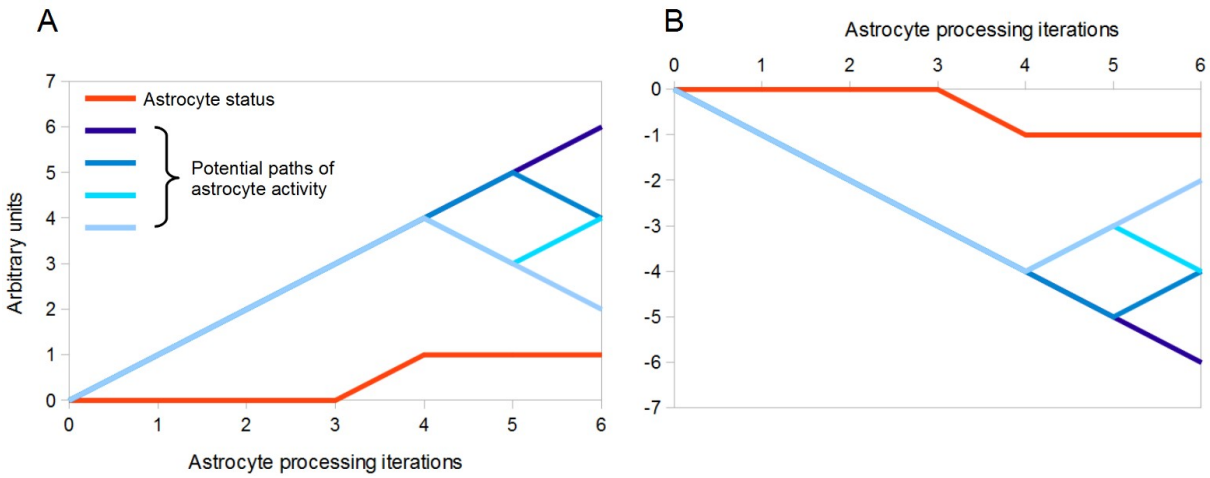

Figure 8 | Astrocyte status invariably follows one of two paths. Astroyte activity inevitably reaches positive or negative threshold (-3 or 3 respectively) thus activating the astrocyte positively or negatively. Once active, the astrocyte remains active for the remaining iterations.

4 – Discussion

The project was split into two main halves: validation of the PPM and the development of the RAP model. The report will now proceed to discuss the validity of these models and what direction future models should take.

4.1 – Porto-Pazos Model

It is worth noting that this project is currently the first public re-implementation of the PPM and is therefore the first third-party validation of this model. The main finding of the simulations of the PPM was that its performance was not significantly better than that of the BNN and the addition of artificial astrocytes did not improve neural network performance. This is surprising as it directly contradicts the results published in (81,82). Comparing the results of this project with that of the original reveals that the performance of my implementation of the PPM was similar to that of the original. Where the two sets of results differ is that my implementation of the underlying BNN significantly outperformed those of the original. Turning to data for learning performance on the Iris dataset, my implementation of the BNN had an average test error score of 5.9% ± 1.98 compared to that of the original which scored 44% ± 4.29 (82). This 44% error is a particularly poor (high) error score given that a native network with random weights achieves 67% error. Although other implementations cannot be compared directly due to variations in certain parameters, it is worth noting that other GA-based implementations achieved error scores as low as 2.1% (97,98).

Taken together, these findings converge on one possible explanation for this discrepancy: the underlying GA implemented in the original publications was in some way partially faulty or restricted. It can be hypothesized that during breeding of the population in the GA, it is the methods of production of variation (crossover and mutation) which are faulty. Such a conclusion would explain why the original BNN stabilized at such a poor error score and why the introduction of the NGA from the PPM increased this performance. Therefore, it is probable that the PPM provided the variation in the population and the good individuals are conserved by the underlying GA. The implications of such conclusions lead us to question the classification of the PPM as a learning rule or as a stochastic

process to produce variation. However, more important than whether artificial astrocytes improve neural network performance is to consider whether the PPM serves as a biologically plausible model of neuron-astrocyte learning networks.

On the surface, the premise of the PPM appears well grounded. The PPM claims to model astroyctes in that they “respond to neurotransmitters released under high synaptic activity and regulate neurotransmission in a larger temporal scale” (81). The findings of the PPM publications are that the learning performance of this astrocyte model improves neural network performance. In the PPM, astrocytes are described as keeping a register of neurons which are constitutively active or inactive and modify synaptic connections accordingly (81,82). However, deeper analysis of the underlying algorithm raises several issues with the representation of astrocytes and the computational logic of the algorithm.

4.1.1 – Temporal scale

The PPM represents the larger temporal scale of astrocyte processing by iterating over the same sample many times, six to be precise. Given the objective of this project, one may overlook unconventional computational methods if they can be justified by biological realism. Having said this, from an AI researcher's perspective, processing the same sample many times is widely-considered as bad practice in machine learning algorithms (89). When one dissects the pattern of activity of astrocytes during these processing iterations (**Fig. 8**), it can be suggested that these processing iterations are superfluous and may be reduced to a single mathematical operation. The first three processing iterations for each sample can be considered redundant since neither the weights nor the inputs to the network will change and therefore the activity values of the neurons will remain identical during these iterations, thus prompting threshold in the astrocytes. The remaining three iterations can be considered redundant since once the astrocyte is activated it will remain active for three iterations regardless of neuronal activity. Therefore, it can be hypothesized that the update of a set of weights can be reduced to a single calculation. For neurons which are activated by the sample, their weights may be multiplied by 1.25^3 (equivalent to 25% increment 3 times) and for neurons which are inactivated by the sample, their weights may be multiplied 0.5^3 (equivalent to 50% decrement 3 times). In conclusion, I suggest that these astrocyte processing iterations lack computational function and can therefore be considered biologically implausible as a representation of temporal scale. Moreover, these excess iterations make the PPM impractical as a pattern recognition or classification tool, due to its speed. As shown by **Fig. 7** the PPM is approximately six times slower than the BNN.

4.1.2 – Astrocyte representation

Having addressed temporal scale, the representation of the astrocytes will now be discussed. In the PPM, each astrocyte is assigned a neuron and its activity is updated in whole integers either positively or negatively dependent on whether the neuron's activity is positive or negative, respectively. This interaction makes two main assumptions untrue of biological astrocytes. Firstly, there is no biological evidence that astrocytes monitor the soma of single neurons in a one-to-one manner. In the brain, astrocytes monitor a unique subset of synapses (26). Secondly, it is biologically implausible to represent the activity of an astrocyte in integers. Astrocyte dynamics are represented in complex Ca^{2+}

waves and therefore should, at a minimal level of abstraction, be represented as continuous values.

However, the greatest oversight of the PPM comes from a failure to address the processing capacity of an astrocyte network. It is highly probable that an important portion of the IP performed by astrocytes in the brain is derived from their own intercommunication (41,43,44,70,99). ANNs have a relatively abstract representation of the internal operations of cells, but in doing so facilitate the exploration of complex network arrangements. The PPM fails to exploit this property of ANNs and therefore automatically fails to serve as an acceptable model.

Another fundamental departure from biology is that astrocytes in the PPM are not actually integrated structures of the network but are instead ephemeral elements employed as part of the algorithm. The output of the network is not dependent on the state of the astrocytes and, in effect, the PPM asserts that astrocytes perform no IP.

4.1.3 – Weight update

In the NGA, positively or negatively activated astrocytes update the weights of their associated neuron by modifying all the weights of that neuron by either 25% or -50%, respectively. There is insufficient biological evidence for such a modification for three main reasons. Firstly, there has been some evidence for the role of astrocytes in synaptic scaling but the probability that the astrocyte modifies the weights of a single neuron is highly improbable. Secondly, astrocytes of the input and output layers modify the same weights as those updated by astrocytes in the hidden layer. This contradicts evidence for astrocytes having distinctly non-overlapping domains (26). Finally, by modelling astrocytes as elements of a learning algorithm, the PPM suggests that astrocytes are the direct mediators of SP. While this may be true in some cases (13,70,100), this is a rather astro-centric view. A more realistic view of SP is that it is a coordinated interplay between astrocytes and neurons and that astrocytes are more likely to gate SP than cause it (50,69,72,74,76).

In summary, the PPM lacks computational efficiency as an optimization algorithm and lacks biological validity in many aspects. Such a conclusion highlights the need for a new model of neuron-astrocyte networks.

4.2 – Reciprocal Astrocyte Processing Model

The RAP model aims to solve many of the issues which emerged in the analysis of the PPM. As mentioned earlier, the results presented for the learning performance of the RAP model should not be taken as definitive results but as preliminary data of the model's performance. These preliminary data show that the RAP model is not capable of being trained by a GA in its current state. Time has limited a full exploration of the model's parameters and full debugging. Nevertheless, the model has a strong biological premise and has promise as a prototype for future models to develop on. I will now discuss the biological validity of the model and what parameters future models should explore.

4.2.1 – Synapse configurations

A principal difference between the PPM and the RAP model is that astrocytes in the RAP model dynamically interact with a subset of synapses rather than associating with a specific neuron. This alone is a vast improvement of biological accuracy, when compared to the PPM. Furthermore, astrocytes monitor distinct subsets of synapses. This property of the network is one of the important

modelling criteria and is strongly supported by biological evidence (26). Associating synapses with astrocytes, however, introduces novel mathematical considerations of permutations. Even in the simplest FFNs such as that of an XOR network (2, 3, 1, input, hidden and output dimensions respectively) there are 6! (720) potential astrocyte-to-synapse configurations (ASCs). Using the dimensions of the above simulations (4, 6, 3) there are 24! (approx. 6.2×10^{23}) potential ASCs. In the current model we initialize the ASC randomly and conserve this configuration throughout the trial. One potentially viable solution may be to include the ASC as a substrate for learning. This would be well supported by biological evidence that astrocytes have plastic domains and variable connectivity (101–106).

In the current RAP model the number of astrocytes is equal to the number of neurons in the hidden layer and the number of synapses monitored by each astrocyte is equal to the number of input neurons. Future models could experiment by modifying the number of astrocytes and the number of synapses per astrocyte. Furthermore, future models need not have just one hidden layer. It may be that inputs require one layer of neuronal abstraction before being processed by astrocytes.

4.2.2 – Lag

As has been emphasized throughout the literature review and the introduction, the temporal scale is a property of astrocytes likely to be important for their role in IP. In the RAP model, astrocyte activation is dependent on residual activation from previous stimuli. This improves on the speed of the network compared to the PPM, as samples are processed sequentially (**Fig. 7**). This is more biologically feasible, as an organism is more likely to be presented with sequentially different stimuli rather than a repeated stimulus.

Residual activation is calculated as the mean of the previous τ iterations is averaged and multiplied by the lag factor γ. For the above simulations τ and γ were arbitrarily set to 3 and 0.1 respectively, however future implementations may wish to experiment with these values. However, perhaps a more biologically plausible variation would be to apply a decay function to each of the previous iterations such that more recent activations will have a greater impact on astrocyte activation than older ones.

4.2.3 – Reciprocal connections

Possibly the most important feature of the RAP model is the reciprocal connections between astrocytes. A lack of an astrocyte network is one of the major downfalls of the PPM. The RAP model represents the connection between two astrocytes by a single weight. The single weight is justified as an abstraction of the proximity and connectivity of the processes belonging to two astrocytes. However, the relationship between a pair of astrocytes is potentially more complex. A simple modification of the RAP model would be to represent the connection between two astrocytes as two separate weights. This would suggest that the ability of astrocyte A to activate astrocyte B can be different from the ability of astrocyte B to activate astrocyte A. Whilst such a relationship is conceivable, there remains to be sufficient experimental evidence for or against such a relationship. From a computational perspective, this modification may also facilitate for better learning as bidirectional weights have the potential to facilitate the modelling of more complex patterns in the dataset.

4.2.4 – Astrocyte representation

As mentioned, an important difference between the RAP model and PPM is that astrocytes in the RAP model output values which are detected by neurons and other astrocytes rather than directly modifying network weights. Input to the astrocyte from presynaptic neuron is detected via $Synout$. Via $Synin$ the output of the astrocyte to the synapse is combined with presynaptic output and detected simultaneously by postsynaptic neuron. $Synout$ represents the probability of this receptor activation causing Ca^{2+} excitability. $Synin$ represents the probability that this Ca^{2+}-based activation causing astrocytic neurotransmitter release. Therefore, by modelling the interaction between astrocyte and synapse with two weights we capitulate the concept of the tripartite synapse (**Fig. 5B**) (6,11). This makes a fundamental departure from the PPM and an important parallel to biology. Astrocytes are no longer ephemeral elements of an algorithm but communicate with neurons in the same currency. The output of the network is now dependent on the state of the astrocytes.

5 – Conclusion

In summary, this project has found that the PPM is not a biologically plausible model of neruo-astrocyte networks for three main reasons. Firstly, the PPM fails to integrate astrocytes into the network and therefore overlooks their role in IP. Secondly, the representation of neuron-astrocyte interaction is ungrounded. Finally, the representation of temporal scale was found to be computationally invalid. Contrasting the authors publications (81,82), the PPM was also found not to improve ANN learning performance. Therefore, this report concludes that one of the pioneering neuron-astrocyte networks should be classified as invalid.

Analysis of the RAP model reveals that, in its current state, it is an unfinished prototype. However, given the scale of this project and the time granted for its completion, this conclusion was somewhat probable. Nevertheless, the RAP has good biological plausibility for three main reasons. Firstly, the RAP model includes tripartite synapses. Secondly, the RAP model allows for interastrocytic communication. Finally, the RAP model engages astrocytes as integrated parts of the network. The RAP model, has therefore made a significant contribution to modelling the brain.

However, as stated, the model remains to be completed. Hopefully the RAP model will form the basis of future projects in an area of neuroscience which desperately calls for the attention of more researchers. This void in neuroscience is epitomised by large scale government funded projects such as the NIH Human Connectome project (107), the BRAIN initiative (108) and Blue Brain project (109). These projects aim to form a comprehensive understanding of the human brain but fail to acknowledge 90% of its cells (18). Whilst the scientists in these projects concede the evident role of astrocytes, the primary objectives of these projects omit astrocytes. Hopefully, the progress made in this project may inspire future research and contribute the development of a model which may cause a paradigm shift.

6 – References

1. Agullo L, Garcia A. Norepinephrine increases cyclic GMP in astrocytes by a mechanism dependent on nitric oxide synthesis. European journal of pharmacology. 1991 Apr 25;206:343–6.

2. Aschner M, Eberle NB, Miller K, Kimelberg HK. Interactions of methylmercury with rat primary astrocyte cultures: inhibition of rubidium and glutamate uptake and induction of swelling. Brain research. 1990 Oct 22;530:245–50.

3. Autillo-Touati A, Rouget M, Araud D, Prochiantz A, Seite R. Astrocyte-regulated GABA-ergic striatal neurons development: an in vitro ultrastructural study. Journal fur Hirnforschung. 1993;34:291–7.

4. Cornell-Bell AH, Finkbeiner SM, Cooper MS, Smith SJ. Glutamate induces calcium waves in cultured astrocytes: long-range glial signaling. Science. 1990 Jan 26;247:470–3.

5. Kimelberg HK, Goderie SK, Higman S, Pang S, Waniewski RA. Swelling-induced release of glutamate, aspartate, and taurine from astrocyte cultures. The Journal of neuroscience : the official journal of the Society for Neuroscience. 1990 May;10:1583–91.

6. Araque A, Parpura V, Sanzgiri RP, Haydon PG. Tripartite synapses: glia, the unacknowledged partner. Trends in neurosciences. 1999 May;22:208–15.

7. Min R, Santello M, Nevian T. The computational power of astrocyte mediated synaptic plasticity. Frontiers in computational neuroscience. 2012;6:93.

8. Araque A. Astrocytes process synaptic information. Neuron glia biology. 2008 Feb;4:3–10.

9. Ben Achour S, Pascual O. Glia: the many ways to modulate synaptic plasticity. Neurochemistry international. 2010 Nov;57:440–5.

10. Kimelberg HK. Receptors on astrocytes--what possible functions? Neurochemistry international. 1995 Jan;26:27–40.

11. Perea G, Navarrete M, Araque A. Tripartite synapses: astrocytes process and control synaptic information. Trends in neurosciences. 2009 Aug;32:421–31.

12. Porter JT, McCarthy KD. Astrocytic neurotransmitter receptors in situ and in vivo. Progress in neurobiology. 1997 Mar;51:439–55.

13. Ben Achour S, Pont-Lezica L, Bechade C, Pascual O. Is astrocyte calcium signaling relevant for synaptic plasticity? Neuron glia biology. 2010 Dec 2;1–9.

14. Dal Pra I, Chiarini A, Nemeth EF, Armato U, Whitfield JF. Roles of Ca2+ and the Ca2+-sensing receptor (CASR) in the expression of inducible NOS (nitric oxide synthase)-2 and its BH4 (tetrahydrobiopterin)-dependent activation in cytokine-stimulated adult human astrocytes. Journal of cellular biochemistry. 2005 Oct 1;96:428–38.

15. De Pitta M, Goldberg M, Volman V, Berry H, Ben-Jacob E. Glutamate regulation of calcium and IP3 oscillating and pulsating dynamics in astrocytes. Journal of biological physics. 2009 Oct;35:383–411.

16. Di Castro MA, Chuquet J, Liaudet N, Bhaukaurally K, Santello M, Bouvier D, et al. Local Ca2+ detection and modulation of synaptic release by astrocytes [Internet]. 2011. Available from: http://www.nature.com/neuro/journal/v14/n10/extref/nn.2929-S4.avi

17. Malarkey EB, Parpura V. Mechanisms of glutamate release from astrocytes. Neurochemistry international. 2008 Jan;52:142–54.

18. Verkhratsky A, Butt A. Glial Neurobiology [Internet]. Chichester, West Sussex: John Wiley & Sons Ltd; 2007. Available from: http://books.google.co.uk/books?id=Fnj1sDax5EsC

19. Zorec R, Araque A, Carmignoto G, Haydon PG, Verkhratsky A, Parpura V. Astroglial excitability and gliotransmission: an appraisal of Ca2+ as a signalling route. ASN neuro [Internet]. 2012;4. Available from: http://www.ncbi.nlm.nih.gov/pubmed/22313347

20. Bennett MV, Contreras JE, Bukauskas FF, Saez JC. New roles for astrocytes: gap junction hemichannels have something to communicate. Trends in neurosciences. 2003 Nov;26:610–7.

21. Dermietzel R. Gap junction wiring: a ‘new’ principle in cell-to-cell communication in the nervous system? Brain research. Brain research reviews. 1998 May;26:176–83.

22. Evans WH, De Vuyst E, Leybaert L. The gap junction cellular internet: connexin hemichannels enter the signalling limelight. The Biochemical journal. 2006 Jul 1;397:1–14.

23. Giaume C, Venance L. Intercellular calcium signaling and gap junctional communication in astrocytes. Glia. 1998 Sep;24:50–64.

24. Saez JC, Retamal MA, Basilio D, Bukauskas FF, Bennett MV. Connexin-based gap junction hemichannels: gating mechanisms. Biochimica et biophysica acta. 2005 Jun 10;1711:215–24.

25. Scemes E, Giaume C. Astrocyte calcium waves: what they are and what they do. Glia. 2006 Nov 15;54:716–25.

26. Bushong EA, Martone ME, Jones YZ, Ellisman MH. Protoplasmic astrocytes in CA1 stratum radiatum occupy separate anatomical domains. The Journal of neuroscience : the official journal of the Society for Neuroscience. 2002 Jan 1;22:183–92.

27. Araque A, Martin ED, Perea G, Arellano JI, Buno W. Synaptically released acetylcholine evokes Ca2+ elevations in astrocytes in hippocampal slices. The Journal of neuroscience : the official journal of the Society for Neuroscience. 2002 Apr 1;22:2443–50.

28. Perea G, Araque A. Properties of synaptically evoked astrocyte calcium signal reveal synaptic information processing by astrocytes. The Journal of neuroscience : the official journal of the Society for Neuroscience. 2005 Mar 2;25:2192–203.

29. Perea G, Araque A. Astrocytes potentiate transmitter release at single hippocampal synapses. Science. 2007 Aug 24;317:1083–6.

30. Grosche J, Matyash V, Moller T, Verkhratsky A, Reichenbach A, Kettenmann H. Microdomains for neuron-glia interaction: parallel fiber signaling to Bergmann glial cells. Nature neuroscience. 1999 Feb;2:139–43.

31. Pearce B, Albrecht J, Morrow C, Murphy S. Astrocyte glutamate receptor activation promotes inositol phospholipid turnover and calcium flux. Neuroscience letters. 1986 Dec 23;72:335–40.

32. Carmignoto G. Reciprocal communication systems between astrocytes and neurones. Progress in Neurobiology. 2000 Dec 15;62(6):561–81.

33. Panatier A, Vallee J, Haber M, Murai KK, Lacaille JC, Robitaille R. Astrocytes are endogenous regulators of basal transmission at central synapses. Cell. 2011 Sep 2;146:785–98.

34. Perea G, Araque A. Synaptic information processing by astrocytes. Journal of physiology, Paris. 2006 Mar;99:92–7.

35. Fiacco TA, McCarthy KD. Intracellular astrocyte calcium waves in situ increase the frequency of spontaneous AMPA receptor currents in CA1 pyramidal neurons. The Journal of neuroscience : the official journal of the Society for Neuroscience. 2004 Jan 21;24:722–32.

36. Parri HR, Crunelli V. Astrocytes, spontaneity, and the developing thalamus. Journal of physiology, Paris. 2002 Apr;96:221–30.

37. Schipke CG, Haas B, Kettenmann H. Astrocytes discriminate and selectively respond to the activity of a subpopulation of neurons within the barrel cortex. Cerebral cortex. 2008 Oct;18:2450–9.

38. Nadkarni S, Jung P, Levine H. Astrocytes optimize the synaptic transmission of information. PLoS computational biology. 2008 May;4:e1000088.

39. Wade J, McDaid L, Harkin J, Crunelli V, Kelso S. Self-repair in a bidirectionally coupled astrocyte-neuron (AN) system based on retrograde signaling. Frontiers in computational neuroscience. 2012;6:76.

40. Bowser DN, Khakh BS. ATP excites interneurons and astrocytes to increase synaptic inhibition in neuronal networks. The Journal of neuroscience : the official journal of the Society for Neuroscience. 2004 Sep 29;24:8606–20.

41. Hoogland TM, Kuhn B, Gobel W, Huang W, Nakai J, Helmchen F, et al. Radially expanding transglial calcium waves in the intact cerebellum. Proceedings of the National Academy of Sciences of the United States of America. 2009 Mar 3;106:3496–501.

42. Sasaki T, Kuga N, Namiki S, Matsuki N, Ikegaya Y. Locally synchronized astrocytes. Cerebral cortex. 2011 Aug;21:1889–900.

43. Hirase H, Qian L, Bartho P, Buzsaki G. Calcium dynamics of cortical astrocytic networks

in vivo. PLoS biology. 2004 Apr;2:E96.

44. Kuga N, Sasaki T, Takahara Y, Matsuki N, Ikegaya Y. Large-scale calcium waves traveling through astrocytic networks in vivo. The Journal of neuroscience : the official journal of the Society for Neuroscience. 2011 Feb 16;31:2607–14.

45. Angulo MC, Kozlov AS, Charpak S, Audinat E. Glutamate released from glial cells synchronizes neuronal activity in the hippocampus. The Journal of neuroscience : the official journal of the Society for Neuroscience. 2004 Aug 4;24:6920–7.

46. Bardoni R, Ghirri A, Zonta M, Betelli C, Vitale G, Ruggieri V, et al. Glutamate-mediated astrocyte-to-neuron signalling in the rat dorsal horn. The Journal of physiology. 2010 Mar 1;588:831–46.

47. Beattie EC, Stellwagen D, Morishita W, Bresnahan JC, Ha BK, Von Zastrow M, et al. Control of synaptic strength by glial TNFalpha. Science. 2002 Mar 22;295:2282–5.

48. Darra E, Ebner FH, Shoji K, Suzuki H, Mariotto S. Dual cross-talk between nitric oxide and D-serine in astrocytes and neurons in the brain. Central nervous system agents in medicinal chemistry. 2009 Dec;9:289–94.

49. Diniz LP, Almeida JC, Tortelli V, Lopes CV, Setti-Perdigao P, Stipursky J, et al. Astrocyte-induced synaptogenesis is mediated by transforming growth factor beta signaling through modulation of D-serine levels in cerebral cortex neurons. The Journal of biological chemistry [Internet]. 2012 Oct 10; Available from: http://www.ncbi.nlm.nih.gov/pubmed/23055518

50. Fossat P, Turpin FR, Sacchi S, Dulong J, Shi T, Rivet JM, et al. Glial D-serine gates NMDA receptors at excitatory synapses in prefrontal cortex. Cerebral cortex. 2012 Mar;22:595–606.

51. Hamilton NB, Attwell D. Do astrocytes really exocytose neurotransmitters? Nature reviews. Neuroscience. 2010 Apr;11:227–38.

52. Hassanpoor H, Fallah A, Raza M. New role for astroglia in learning: Formation of muscle memory. Medical hypotheses [Internet]. 2012 Sep 17; Available from: http://www.ncbi.nlm.nih.gov/pubmed/22995586

53. Kang J, Jiang L, Goldman SA, Nedergaard M. Astrocyte-mediated potentiation of inhibitory synaptic transmission. Nature neuroscience. 1998 Dec;1:683–92.

54. Mothet JP, Pollegioni L, Ouanounou G, Martineau M, Fossier P, Baux G. Glutamate receptor activation triggers a calcium-dependent and SNARE protein-dependent release of the gliotransmitter D-serine. Proceedings of the National Academy of Sciences of the United States of America. 2005 Apr 12;102:5606–11.

55. Anderson CM, Swanson RA. Astrocyte glutamate transport: review of properties, regulation, and physiological functions. Glia. 2000 Oct;32(1):1–14.

56. Diamond JS, Bergles DE, Jahr CE. Glutamate release monitored with astrocyte transporter currents during LTP. Neuron. 1998 Aug;21:425–33.

57. Araque A, Parpura V, Sanzgiri RP, Haydon PG. Glutamate-dependent astrocyte modulation of synaptic transmission between cultured hippocampal neurons. The European journal of neuroscience. 1998 Jun;10:2129–42.

58. Fellin T, Pascual O, Gobbo S, Pozzan T, Haydon PG, Carmignoto G. Neuronal synchrony mediated by astrocytic glutamate through activation of extrasynaptic NMDA receptors. Neuron. 2004 Sep 2;43:729–43.

59. Golech SA, McCarron RM, Chen Y, Bembry J, Lenz F, Mechoulam R, et al. Human brain endothelium: coexpression and function of vanilloid and endocannabinoid receptors. Brain research. Molecular brain research. 2004 Dec 6;132:87–92.

60. Liu QS, Xu Q, Arcuino G, Kang J, Nedergaard M. Astrocyte-mediated activation of neuronal kainate receptors. Proceedings of the National Academy of Sciences of the United States of America. 2004 Mar 2;101:3172–7.

61. Navarrete M, Araque A. Endocannabinoids mediate neuron-astrocyte communication. Neuron. 2008 Mar 27;57:883–93.

62. Shigetomi E, Bowser DN, Sofroniew MV, Khakh BS. Two forms of astrocyte calcium excitability have distinct effects on NMDA receptor-mediated slow inward currents in pyramidal neurons. The Journal of neuroscience : the official journal of the Society for Neuroscience. 2008 Jun 25;28:6659–63.

63. Parri HR, Gould TM, Crunelli V. Spontaneous astrocytic Ca2+ oscillations in situ drive NMDAR-mediated neuronal excitation. Nature neuroscience. 2001 Aug;4:803–12.

64. D'Ascenzo M, Fellin T, Terunuma M, Revilla-Sanchez R, Meaney DF, Auberson YP, et al. mGluR5 stimulates gliotransmission in the nucleus accumbens. Proceedings of the National Academy of Sciences of the United States of America. 2007 Feb 6;104:1995–2000.

65. Jourdain P, Bergersen LH, Bhaukaurally K, Bezzi P, Santello M, Domercq M, et al. Glutamate exocytosis from astrocytes controls synaptic strength. Nature neuroscience. 2007 Mar;10:331–9.

66. Navarrete M, Araque A. Endocannabinoids potentiate synaptic transmission through stimulation of astrocytes. Neuron. 2010 Oct 6;68:113–26.

67. Pascual O, Casper KB, Kubera C, Zhang J, Revilla-Sanchez R, Sul JY, et al. Astrocytic purinergic signaling coordinates synaptic networks. Science. 2005 Oct 7;310:113–6.

68. Zhang JM, Wang HK, Ye CQ, Ge W, Chen Y, Jiang ZL, et al. ATP released by astrocytes mediates glutamatergic activity-dependent heterosynaptic suppression. Neuron. 2003 Dec 4;40:971–82.

69. Henneberger C, Papouin T, Oliet SH, Rusakov DA. Long-term potentiation depends on release of D-serine from astrocytes. Nature. 2010 Jan 14;463:232–6.

70. Navarrete M, Perea G, Fernandez de Sevilla D, Gomez-Gonzalo M, Nunez A, Martin ED, et al. Astrocytes mediate in vivo cholinergic-induced synaptic plasticity. PLoS biology. 2012 Feb;10:e1001259.

71. Takata N, Mishima T, Hisatsune C, Nagai T, Ebisui E, Mikoshiba K, et al. Astrocyte calcium signaling transforms cholinergic modulation to cortical plasticity in vivo. The Journal of neuroscience : the official journal of the Society for Neuroscience. 2011 Dec 7;31:18155–65.

72. Yang Y, Ge W, Chen Y, Zhang Z, Shen W, Wu C, et al. Contribution of astrocytes to hippocampal long-term potentiation through release of D-serine. Proceedings of the National Academy of Sciences of the United States of America. 2003 Dec 9;100:15194–9.

73. Ho JM, Smith NS, Adams SA, Bradshaw HB, Demas GE. Photoperiodic changes in endocannabinoid levels and energetic responses to altered signalling at CB1 receptors in Siberian hamsters. Journal of neuroendocrinology. 2012 Jul;24:1030–9.

74. Kakegawa W, Miyoshi Y, Hamase K, Matsuda S, Matsuda K, Kohda K, et al. D-serine regulates cerebellar LTD and motor coordination through the delta2 glutamate receptor. Nature neuroscience. 2011 May;14:603–11.

75. Zhang J, Chen C. Endocannabinoid 2-arachidonoylglycerol protects neurons by limiting COX-2 elevation. The Journal of biological chemistry. 2008 Aug 15;283:22601–11.

76. Molnar E. Long-term potentiation in cultured hippocampal neurons. Seminars in cell & developmental biology. 2011 Jul;22:506–13.

77. Rison RA, Stanton PK. Long-term potentiation and N-methyl-D-aspartate receptors: foundations of memory and neurologic disease? Neuroscience and biobehavioral reviews. 1995 Winter;19:533–52.

78. Mothet JP, Parent AT, Wolosker H, Brady RO, Linden DJ, Ferris CD, et al. D-serine is an endogenous ligand for the glycine site of the N-methyl-D-aspartate receptor. Proceedings of the National Academy of Sciences of the United States of America. 2000 Apr 25;97:4926–31.

79. Oberheim NA, Takano T, Han X, He W, Lin JH, Wang F, et al. Uniquely hominid features of adult human astrocytes. The Journal of neuroscience : the official journal of the Society for Neuroscience. 2009 Mar 11;29:3276–87.

80. Han X, Chen M, Wang F, Windrem M, Wang S, Shanz S, et al. Forebrain Engraftment by Human Glial Progenitor Cells Enhances Synaptic Plasticity and Learning in Adult Mice. Cell Stem Cell. 2013 Mar 7;12(3):342–53.

81. Porto-Pazos AB, Veiguela N, Mesejo P, Navarrete M, Alvarellos A, Ibanez O, et al. Artificial astrocytes improve neural network performance. PloS one. 2011;6:e19109.

82. Alvarellos-Gonzalez A, Pazos A, Porto-Pazos AB. Computational models of neuron-astrocyte interactions lead to improved efficacy in the performance of neural networks. Computational and mathematical methods in medicine. 2012;2012:476324.

83. Kuhn TS. The Structure of Scientific Revolutions. New ed of 3 Revised ed. University of Chicago Press; 1996.

84. Atiya A, Talaat N, Shaheen S. An efficient stock market forecasting model using neural

networks. , International Conference on Neural Networks,1997. 1997. p. 2112–2115 vol.4.

85. Kuah K, Bodruzzaman M, Zein-Sabatto S. A neural network-based text independent voice recognition system. , Proceedings of the 1994 IEEE Southeastcon ’94. Creative Technology Transfer - A Global Affair. 1994. p. 131–5.

86. El-Khamy SE, Abdel-Alim OA, Saii MM. Neural network face recognition using statistical feature and skin texture parameters. Radio Science Conference, 2001. NRSC 2001. Proceedings of the Eighteenth National. 2001. p. 233–240 vol.1.

87. Safaric R, Jezernik K, Rodic M, Sabanovic A, Uran S. Sliding-mode neural network robot controller. , 1996 4th International Workshop on Advanced Motion Control, 1996. AMC ’96-MIE. Proceedings. 1996. p. 395–400 vol.1.

88. Yong SL, Hagenbuchner M, Tsoi AC. Ranking Web Pages Using Machine Learning Approaches. IEEE/WIC/ACM International Conference on Web Intelligence and Intelligent Agent Technology, 2008. WI-IAT ’08. 2008. p. 677–80.

89. Haykin SO. Neural Networks and Learning Machines. 3rd ed. Prentice Hall; 2008.

90. Fisher RA. The Use of Multiple Measurements in Taxonomic Problems. Annals of Eugenics. 1936;7(2):179–88.

91. Hodgkin AL, Huxley AF. A quantitative description of membrane current and its application to conduction and excitation in nerve. J Physiol. 1952 Aug 28;117(4):500–44.

92. William P. Bellingham KG-B. Summation and configuration in patterning schedules with the rat and rabbit. 1985;13(2):152–64.

93. Storkey AJ, Valabregue R. The basins of attraction of a new Hopfield learning rule. Neural Netw. 1999 Jul;12(6):869–76.

94. Schmidhuber J, Wierstra D, Gagliolo M, Gomez F. Training recurrent networks by Evolino. Neural Comput. 2007 Mar;19(3):757–79.

95. Hinton GE, Osindero S, Teh Y-W. A fast learning algorithm for deep belief nets. Neural Comput. 2006 Jul;18(7):1527–54.

96. Goldberg DE. Genetic Algorithms in Search, Optimization, and Machine Learning. 1st ed. Addison-Wesley Professional; 1989.

97. Demiriz A, Bennett KP, Embrechts MJ. A Genetic Algorithm Approach for Semi-Supervised Clustering. International Journal of Smart Engineering System Design. 2002;4(1):21–30.

98. Eggermont J, Kok JN, Kosters WA. Genetic Programming for data classification: partitioning the search space. Proceedings of the 2004 ACM symposium on Applied computing [Internet]. New York, NY, USA: ACM; 2004 [cited 2013 Apr 28]. p. 1001–5. Available from: http://doi.acm.org/10.1145/967900.968104

99. Dani JW, Chernjavsky A, Smith SJ. Neuronal activity triggers calcium waves in

hippocampal astrocyte networks. Neuron. 1992 Mar;8:429–40.

100. Gordon GR, Iremonger KJ, Kantevari S, Ellis-Davies GC, MacVicar BA, Bains JS. Astrocyte-mediated distributed plasticity at hypothalamic glutamate synapses. Neuron. 2009 Nov 12;64:391–403.

101. Lavialle M, Aumann G, Anlauf E, Prols F, Arpin M, Derouiche A. Structural plasticity of perisynaptic astrocyte processes involves ezrin and metabotropic glutamate receptors. Proceedings of the National Academy of Sciences of the United States of America. 2011 Aug 2;108:12915–9.

102. Oliet SH, Piet R, Poulain DA. Control of glutamate clearance and synaptic efficacy by glial coverage of neurons. Science. 2001 May 4;292:923–6.

103. Sosinsky GE, Nicholson BJ. Structural organization of gap junction channels. Biochimica et biophysica acta. 2005 Jun 10;1711:99–125.

104. Theodosis DT, Poulain DA, Oliet SH. Activity-dependent structural and functional plasticity of astrocyte-neuron interactions. Physiological reviews. 2008 Jul;88:983–1008.

105. Ventura R, Harris KM. Three-dimensional relationships between hippocampal synapses and astrocytes. The Journal of neuroscience : the official journal of the Society for Neuroscience. 1999 Aug 15;19:6897–906.

106. Witcher MR, Kirov SA, Harris KM. Plasticity of perisynaptic astroglia during synaptogenesis in the mature rat hippocampus. Glia. 2007 Jan 1;55:13–23.

107. Toga AW, Clark KA, Thompson PM, Shattuck DW, Van Horn JD. Mapping the Human Connectome. Neurosurgery. 2012 Jul;71(1):1–5.

108. Alivisatos AP, Chun M, Church GM, Greenspan RJ, Roukes ML, Yuste R. The Brain Activity Map Project and the Challenge of Functional Connectomics. Neuron. 2012 Jun;74(6):970–4.

109. Markram H. The Blue Brain Project. Nat Rev Neurosci. 2006 Feb;7(2):153–60.

110. Furber S, Temple S. Neural systems engineering. J. R. Soc. Interface. 2007 Apr 22;4(13):193–206.